

# Reinforcement of EPDM-based ionic thermoplastic elastomer by carbon black

Thomas Kurian, P. P. De, D. Khastgir, D. K. Tripathy and S. K. De\*

Rubber Technology Center, Indian Institute of Technology, Kharagpur 721302, India

and D. G. Peiffer

Exxon Research & Engineering Company, Route 22 East, Clinton Township, NJ 08801, USA

(Received 8 December 1994)

High abrasion furnace carbon black improves the physical properties of zinc sulfonated ethylene–propylene–diene terpolymer of high (75 wt%) ethylene content. Properties studied include hardness, stress–strain characteristics, tear strength, hysteresis and abrasion resistance. Scanning electron photomicrographs of the tear fractured and abraded surfaces show changes in failure mode of the polymer on incorporation of carbon black. Results of dynamic mechanical analyses and dielectric thermal analyses show that carbon black reinforces the ionomers, presumably through weak rubber–filler interaction involving the backbone chains and strong interaction between the active sites of the filler surface and the ionic aggregates present in the ‘multiplets’ and ‘clusters’. Reprocessability studies in the Monsanto Processability Tester (MPT) show that the carbon black filled polymer can be reprocessed like a thermoplastic elastomer and there was no fall in properties even after three cycles of extrusion through the MPT.

(Keywords: carbon black; zinc sulfonated EPDM; physical properties)

## INTRODUCTION

Thermoplastic elastomers based on ionomers have recently emerged as materials of great potential<sup>1–5</sup>. Zinc salt of sulfonated ethylene–propylene–diene terpolymer (EPDM) of high ethylene content is an example of an ionic thermoplastic elastomer<sup>3,4</sup>. While studying the effect of fillers on the properties of this material, we observed an improvement in the physical properties on incorporation of high abrasion furnace (HAF) carbon black. This paper reports the results of studies on the effect of HAF carbon black on the physical properties and processability of zinc sulfonated EPDM with 75 wt% ethylene content.

## EXPERIMENTAL

Polymers used in this study were: (i) thermoplastic EPDM containing 75% ethylene, 20% propylene and 5% 5-ethylidene-2-norbornene, and (ii) zinc salt of sulfonated ethylene–propylene–diene terpolymer formed by sulfonation of the pendent unsaturation in the thermoplastic EPDM, followed by neutralization of the resultant EPDM sulfonic acid using the procedure described by Makowski *et al.*<sup>6</sup>. The level of sulfonation in zinc sulfonated EPDM was 30 meq/100 g polymer. Both the polymers were supplied by Exxon Research & Engineering Company, NJ, USA. The carbon black used was high abrasion furnace type (N-330 grade; surface area 80 m<sup>2</sup> g<sup>−1</sup>; pH 7.6), supplied by Phillips Carbon Black Ltd, Durgapur, India.

Rubber was mixed with carbon black filler in a Brabender Plasticorder (model PLE-330) using a cam-type rotor for 6 min at a rotor speed of 80 rev min<sup>−1</sup> at 150°C. The neat polymers were masticated under the same conditions. Test specimens were prepared by moulding in an electrically heated hydraulic press for 5 min at 160°C under a pressure of 10 MPa.

The hardness was determined as per ASTM D2240 (1986) and expressed in Shore A units. The stress–strain properties were determined at 25, 50 and 70°C according to ASTM D412 (1987) using dumb-bell specimens in a Zwick Universal Testing Machine (UTM; model 1445) fitted with a temperature controlled cabinet using a crosshead speed of 500 mm min<sup>−1</sup>. The tension set at 200% elongation was determined as per ASTM D412 (1987). The tear resistance was determined as per ASTM D624 (1986) using unnicked 90° angle test-pieces (die C) at 25°C at a crosshead speed of 500 mm min<sup>−1</sup> in the Zwick UTM. The hysteresis loss was determined according to ASTM D412 (1980) by stretching dumb-bell specimens to a strain level of 200%. The abrasion resistance was determined in a Du Pont Abrasion Tester (BS 903: Part A9 1957 method C) and expressed as abrasion loss, which is the volume in cm<sup>3</sup> abraded from a test specimen per hour.

The tear fractured surface and the abraded surfaces were sputter-coated with gold within 24 h of testing and examined under a Cam Scan scanning electron microscope (series 2DV).

Dynamic mechanical analyses were performed in a Rheovibron DDV-III-EP Viscoelastometer at a frequency of 3.5 Hz and a strain amplitude of 0.0025 cm.

\* To whom correspondence should be addressed

**Table 1** Physical properties at room temperature

Sample	Hardness (Shore A)	Modulus at 300% elongation (MPa)	Tensile strength (MPa)	Elongation at break (%)	Tear strength (kN m <sup>-1</sup> )	Hysteresis loss (J m <sup>-2</sup> × 10 <sup>3</sup> )	Tension set at 200% elongation (%)	Abrasion loss (cm <sup>3</sup> h <sup>-1</sup> )
EPDM	56	2.7	11.0	1036	63	82	46	0.29
Zinc sulfonated EPDM (SE)	69	7.3	23.0	691	115	146	35	0.21
SE + 10 phr filler	70	9.6	21.1	526	116	210	34	0.18
SE + 20 phr filler	75	12.9	22.5	494	144	265	32	0.14
SE + 35 phr filler	77	18.8	22.4	378	164	421	30	0.13

The measurements were carried out over a temperature range of  $-100$  to  $200^{\circ}\text{C}$  at a heating rate of  $1^{\circ}\text{C min}^{-1}$ .

Dielectric thermal analyses were carried out in a Du Pont DEA 2970 Dielectric Analyser in nitrogen environment. Square specimens of 25 mm side and 0.5 mm thickness were used. The measurements were carried out over a frequency range of 1 to 100 000 Hz and a temperature range of 20 to  $200^{\circ}\text{C}$  at a heating rate of  $5^{\circ}\text{C min}^{-1}$ .

The processability studies were carried out by using a Monsanto Processability Tester (MPT) at shear rates of 36, 90, 181 and  $289\text{ s}^{-1}$  and a temperature of  $170^{\circ}\text{C}$ . The capillary length (29.77 mm) to diameter (1.50 mm) ratio was 20, with an entrance angle of  $45$  and  $60^{\circ}$  (compound). The preheat time for each sample was 5 min.

The reprocessability of the polymer was tested by extruding the sample in the MPT at  $160^{\circ}\text{C}$ , at a shear rate of  $18\text{ s}^{-1}$ ; the extrudate was re-extruded under similar conditions and the process was repeated up to three cycles. Before each extrusion the sample was preheated in the barrel of the MPT at  $160^{\circ}\text{C}$  for 10 min. Apparent viscosity and apparent shear stress after each cycle were noted. The extrudate sample after each cycle was allowed to rest for 24 h before the tensile strength was measured.

## RESULTS AND DISCUSSION

The physical properties of the neat polymers and HAF carbon black filled zinc sulfonated EPDM compounds are summarized in Table 1. Zinc sulfonated EPDM showed higher hardness than thermoplastic EPDM. Hardness is a measure of modulus of elasticity at low strain<sup>7</sup>. The increase in modulus of elasticity by ionic aggregates in zinc sulfonated EPDM may be the reason for its higher hardness. As expected, the hardness of zinc sulfonated EPDM was found to increase as the carbon black loading increased.

The stress-strain behaviour of EPDM, zinc sulfonated EPDM and the compounds of zinc sulfonated EPDM containing 10, 20 and 35 phr of carbon black filler at 25, 50 and  $70^{\circ}\text{C}$  is shown in Figure 1. At room temperature zinc sulfonated EPDM showed higher modulus and tensile strength and lower elongation at break than EPDM, owing to the presence of ionic domains which act as physical crosslinks<sup>8</sup>. Incorporation of filler causes a gradual increase in modulus and decreases in elongation at break, but the tensile strength remains almost constant. Although the modulus and tensile strength of the corresponding thermoplastic EPDM, used as control, dropped drastically at higher test temperatures, zinc sulfonated EPDM showed greater retention of the

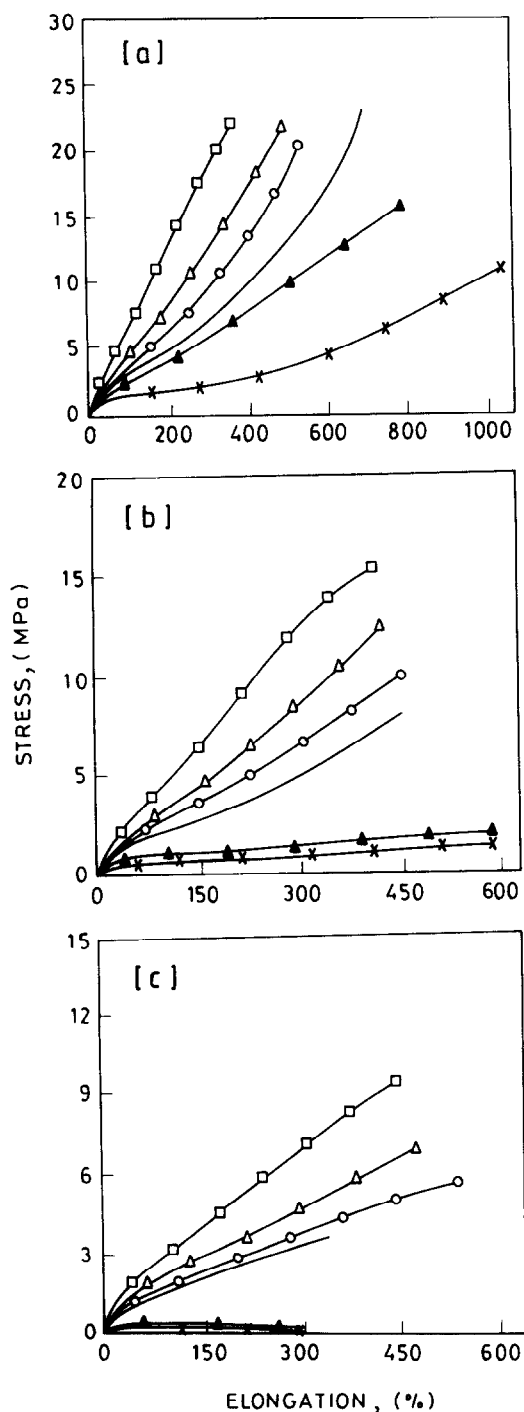


**Figure 1** Stress-strain plots of EPDM (×), EPDM + 35 phr filler (▲), zinc sulfonated EPDM (—), zinc sulfonated EPDM + 10 phr filler (○), zinc sulfonated EPDM + 20 phr filler (△) and zinc sulfonated EPDM + 35 phr filler (□) at (a)  $25^{\circ}\text{C}$ , (b)  $50^{\circ}\text{C}$  and (c)  $70^{\circ}\text{C}$

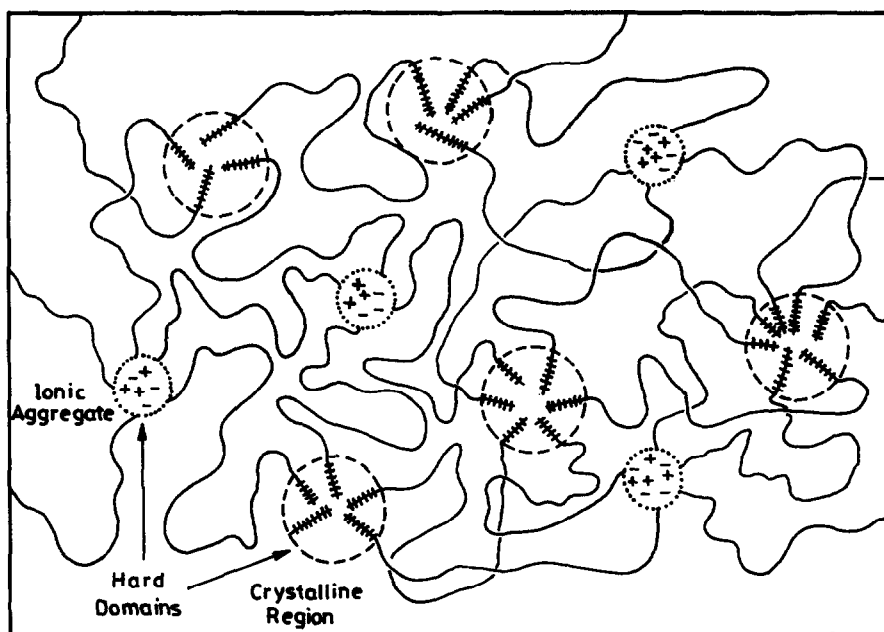


Figure 2 Schematic morphological structure of zinc sulfonated EPDM containing 75 wt% ethylene

properties at elevated testing temperatures, the retention being higher in the presence of carbon black (Figure 1). In contrast to zinc sulfonated EPDM, the control thermoplastic EPDM does not contain any physical crosslinks and thus the retention of properties at higher test temperatures is low. The morphological structure of zinc sulfonated EPDM is believed to be similar to that of conventional thermoplastic elastomers, i.e. a combination of hard domains and soft segments as depicted in Figure 2. The hard domains may consist both of crystallites due to polyethylene blocks and ionic aggregates due to metal sulfonate groups. In the case of zinc sulfonated EPDM, incorporation of carbon black filler seems to strengthen the physical crosslinks arising from the ionic aggregates, as elaborated later in this paper, thereby increasing the high temperature strength properties. For the same reasons, tension set values (Table 1) gradually decreased with increase in filler loading. Incorporation of carbon black in EPDM increases the room temperature stress-strain properties due to weak rubber-filler interaction, but at higher test temperatures the properties drop sharply. This is in sharp contrast to the observation made with carbon black filled zinc sulfonated EPDM.

Zinc sulfonated EPDM showed higher tear strength

than the control thermoplastic EPDM. Tear resistance of elastomers is a measure of crack propagation. It is known that tear strength is enhanced by factors which tend to dissipate energy<sup>9</sup>. The ionic domains of zinc sulfonated EPDM may be acting as tear deviators or arrestors. Figure 3 shows scanning electron photomicrographs of tear fractured surfaces. The fracturograph of thermoplastic EPDM (Figure 3a) exhibited a single straight tear line which propagated from one end to the other in a stick-slip manner. Occurrence of a straight tear path in a smooth surface is an indication of low tear strength<sup>10</sup>. Zinc sulfonated EPDM, on the other hand, shows multiple tear lines propagating in stick-slip manner (Figure 3b). This may be due to the deviation of the tear path caused by the ionic aggregates and accounts for the two-fold increase in tear strength of zinc sulfonated EPDM compared with the thermoplastic EPDM. Incorporation of carbon black caused further deviation in tear path, producing knotty tear (Figure 3c) and thereby causing further improvement in the strength. Results of hysteresis studies are shown in Figure 4. Areas under the hysteresis loop run parallel with the tear strength. Zinc sulfonated EPDM shows higher hysteresis than the thermoplastic EPDM due to the additional energy dissipation mechanisms in the former, arising

Table 2 Results of dynamic mechanical analysis

Sample	$T_g^a$ (°C)	Tan $\delta$ at $T_g$	Transition due to ionic aggregates <sup>b</sup> , $T_i$ (°C)	Tan $\delta$ at $T_i$	Transition due to melting of crystallites <sup>b</sup> (°C)	Storage modulus $E'$ at 25°C (MPa)
EPDM	-26	0.365	—	—	<sup>c</sup>	11.0
Zinc sulfonated EPDM (SE)	-26	0.257	27 to 80	0.040	119	19.8
SE + 10 phr filler	-26	0.232	31 to 62	0.044	115	22.0
SE + 20 phr filler	-26	0.203	31 to 68	0.054	117	34.0
SE + 35 phr filler	-26	0.194	33 to 62	0.055	116	39.3

<sup>a</sup> From  $(\tan \delta)_{\max}$  in the plot of  $\tan \delta$  versus temperature

<sup>b</sup> From  $\tan \delta$  versus temperature plot

<sup>c</sup> Not detectable

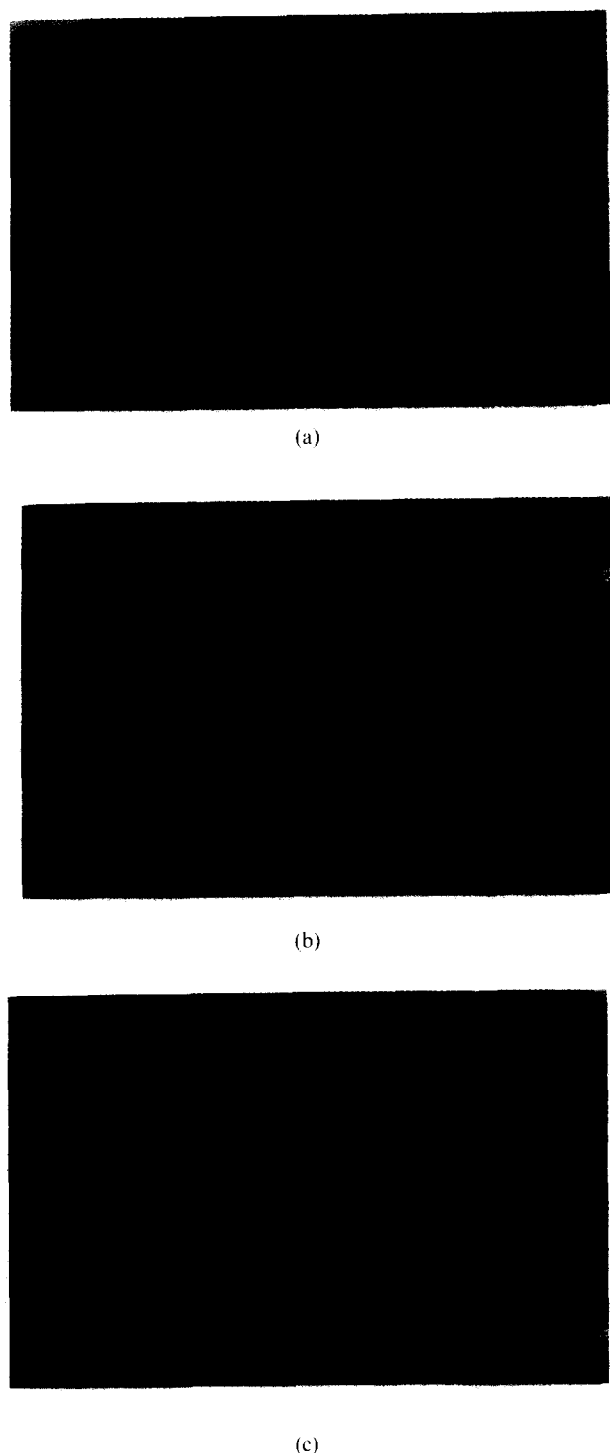


**Figure 3** Scanning electron photomicrographs of tear fractured surfaces: (a) EPDM, (b) zinc sulfonated EPDM and (c) zinc sulfonated EPDM + 20 phr filler

from the ionic aggregates which may be considered to behave as ultrafine reinforcing filler particles in the host polymer, in addition to acting as multifunctional cross-links<sup>9,11</sup>. The hysteresis of zinc sulfonated EPDM was found to increase with the incorporation of the carbon black, gradually increasing as the loading of the filler increased. The increase in hysteresis on addition of filler is due to additional energy dissipation mechanisms, such as motion of filler particles, chain slippage or breakage,

and dewetting at high strains<sup>9</sup>. Additional energy dissipation in zinc sulfonated EPDM and its carbon black filled compounds may be the reason for their higher tear strength. Abrasion resistance also follows the same pattern as the tear strength.

Figure 5 shows scanning electron photomicrographs of abraded surfaces. The wear fractograph of the control thermoplastic EPDM (Figure 5a) shows vertical ridges, in a direction perpendicular to the direction of abrasion, which is characteristic of the frictional type of wear<sup>12</sup>. Schallamach observed similar ridge formation on the worn surfaces of natural rubber<sup>13</sup>. In the case of zinc sulfonated EPDM (Figure 5b), the ridge spacing decreased and scratches appeared on the surface in the direction of abrasion. This shows the change in mechanism of abrasion with the introduction of ionic moieties in EPDM. With the incorporation of carbon black filler (Figure 5c), the ridges disappeared and the mechanics of abrasion changed to abrasive wear in which the scratches are formed in the direction of abrasion, showing low abrasion loss<sup>14</sup>.

Results of dynamic mechanical analyses are summarized in Table 2. Zinc sulfonated EPDM showed higher storage modulus than the control EPDM. Incorporation of carbon black increased the storage modulus of zinc sulfonated EPDM. The reinforcement of zinc sulfonated EPDM by carbon black is evident from the linear plot of  $E'_f/E'_g$  versus volume fraction of the filler ( $\phi$ ) (Figure 6), which could be represented by the relation:

$$E'_f/E'_g = 1 + 6.9\phi \quad (1)$$

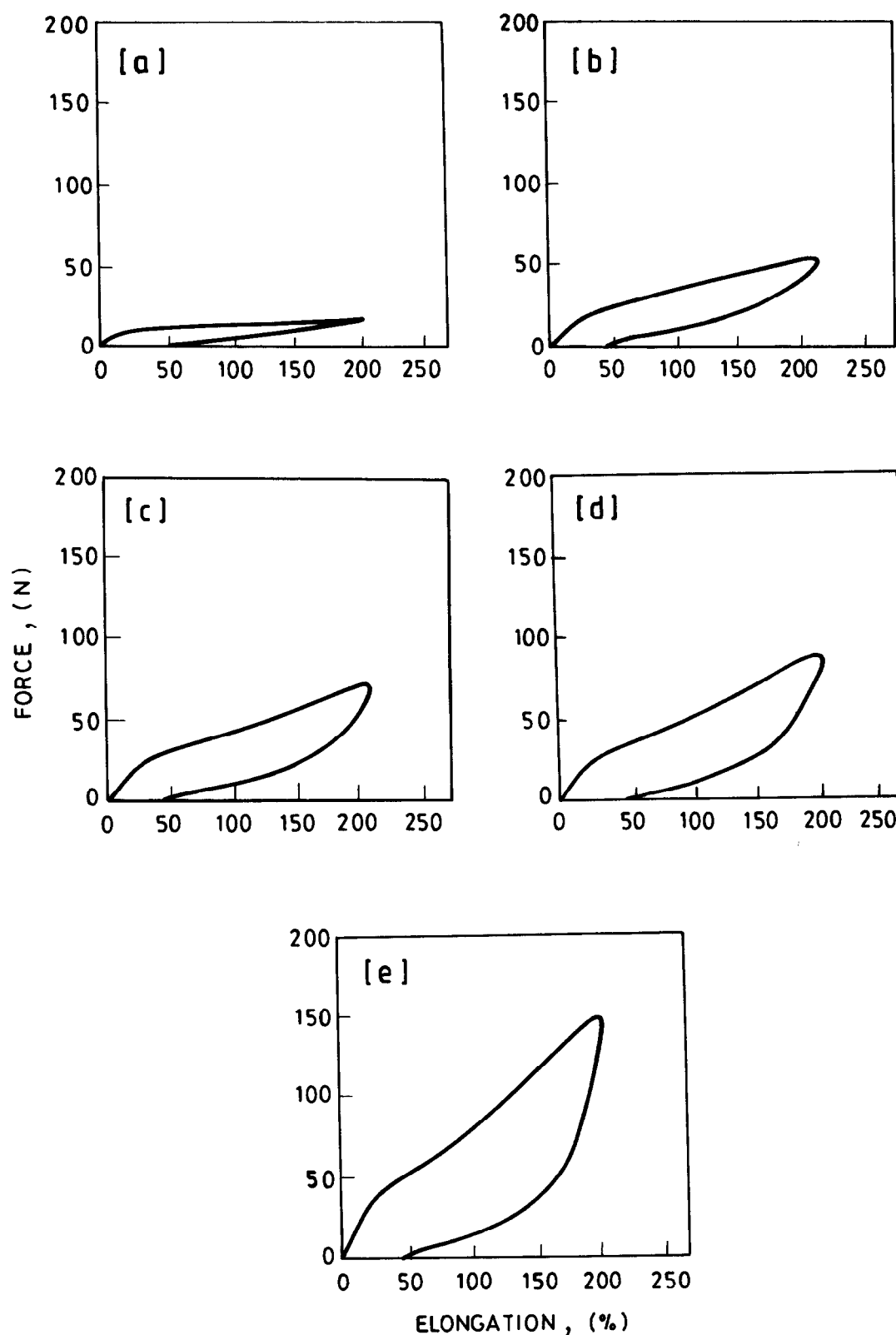
where  $E'_f$  is the storage modulus of the filled compound and  $E'_g$  is the storage modulus of the neat zinc sulfonated EPDM at 25°C. This is very similar to the relationship proposed by Smallwood in the case of diene rubbers<sup>15</sup>.

Figure 7 shows the variation of loss tangent ( $\tan \delta$ ) with temperature for EPDM, and the compounds of zinc sulfonated EPDM containing HAF carbon black. The glass-rubber transition ( $T_g$ ) occurs around -26°C in all cases. The  $\tan \delta_{\max}$  (that is, the  $\tan \delta$  value at  $T_g$ ) was less in the case of zinc sulfonated EPDM than in EPDM. This is because of the stiffening imparted by the ionic domains in zinc sulfonated EPDM<sup>16</sup>. Incorporation of HAF carbon black causes lowering of  $\tan \delta_{\max}$  of the zinc sulfonated EPDM due to strong rubber-filler interaction involving the backbone chains. Figure 8 shows the plot of  $(\tan \delta_{\max})_f/(\tan \delta_{\max})_g$  versus volume fraction of the filler ( $\phi$ ). Here f stands for the filled system and g denotes the neat zinc sulfonated EPDM. The results could be fitted with the following relation:

$$(\tan \delta_{\max})_f/(\tan \delta_{\max})_g = 1 - 2.8\phi + 7.6\phi^2 \quad (2)$$

The plot is similar to that obtained in the case of conventional rubber systems with strong rubber-filler interaction<sup>17</sup>.

Apart from  $T_g$ , zinc sulfonated EPDM and its carbon black filled compounds show two other transitions: one around 119°C, which is believed to be due to the melting of the crystalline zone of the polyethylene block, and another broad transition in the temperature range of 27 to 80°C<sup>18</sup>, which is ascribed to the transition due to the ionic aggregates ( $T_i$ ). In the case of the rubbery ionomers, the transition due to ionic groups has been found to occur in the same temperature range as

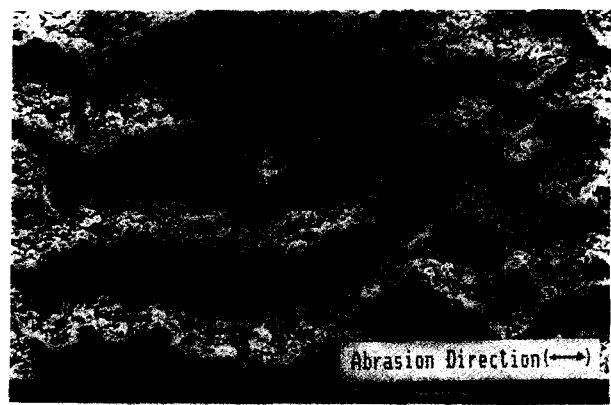


**Figure 4** Hysteresis plots of (a) EPDM, (b) zinc sulfonated EPDM, (c) zinc sulfonated EPDM + 10 phr filler, (d) zinc sulfonated EPDM + 20 phr filler and (e) zinc sulfonated EPDM + 35 phr filler

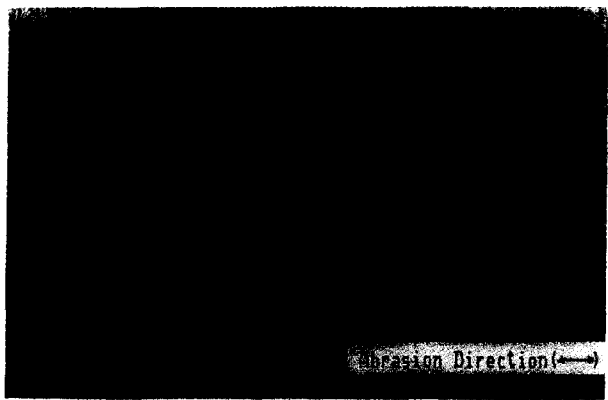
observed here<sup>2,19</sup>. It has been reported earlier that in the case of crystalline ionomers transition due to ionic aggregates occurs at a lower temperature than the crystalline melting temperature<sup>20–22</sup>. In the case of EPDM, the broad transition due to the ionic aggregates has not been observed and also the high temperature transition due to the crystalline zone could not be

detected owing to softening of the test sample above 100°C. However, the presence of ionic aggregates in zinc sulfonated EPDM makes the matrix rigid enough for the crystalline melting zone to be detected.

Incorporation of filler increased the  $\tan \delta$  value at the high temperature ionic transition ( $T_i$ ). The  $\tan \delta$  value at  $T_i$  increased as the loading of carbon black increased.



(a)



(b)



(c)

**Figure 5** Scanning electron photomicrographs of abraded surfaces: (a) EPDM, (b) zinc sulfonated EPDM and (c) zinc sulfonated EPDM + 20 phr filler

Figure 8 shows the variation of  $(\tan \delta)_f/(\tan \delta)_g$  versus the volume fraction of the filler ( $\phi$ ). The results could be fitted to the following relation:

$$(\tan \delta)_f/(\tan \delta)_g = 1 + 4.3\phi - 10.2\phi^2 \quad (3)$$

From the above results it can be inferred that the rubber–filler interaction in the case of the carbon black filled zinc sulfonated EPDM is of two types: (a) the interaction between the filler particles and the non-polar

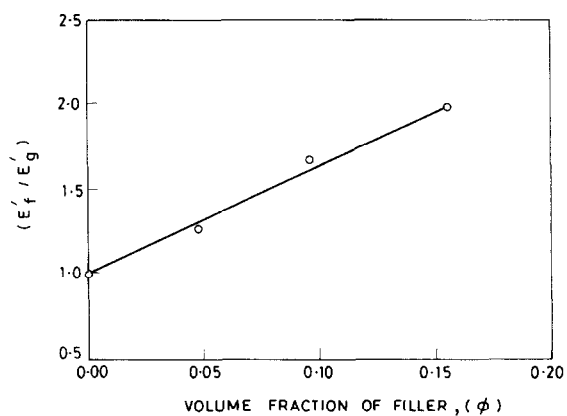


**Figure 6** Effect of volume fraction of HAF carbon black on the relative storage modulus of zinc sulfonated EPDM

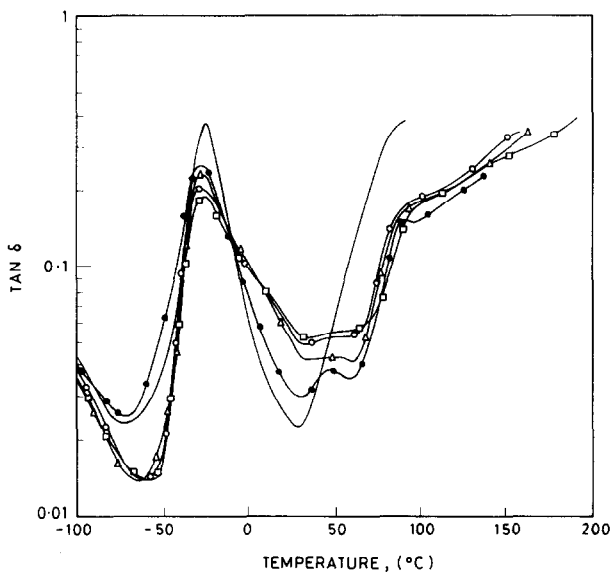


**Figure 7** Semilogarithmic plots of  $\tan \delta$  versus temperature of EPDM (—), zinc sulfonated EPDM ( $\bullet$ ), zinc sulfonated EPDM + 10 phr filler ( $\Delta$ ), zinc sulfonated EPDM + 20 phr filler ( $\circ$ ) and zinc sulfonated EPDM + 35 phr filler ( $\square$ )

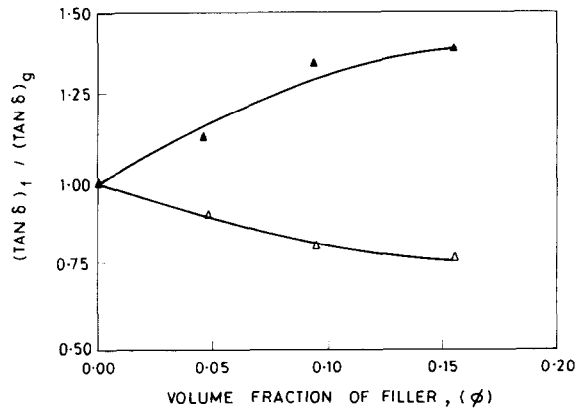


**Figure 8** Effect of volume fraction of HAF carbon black on the relative  $\tan \delta$  value of zinc sulfonated EPDM, at  $T_g$  ( $\Delta$ ) and at  $T_i$  ( $\blacktriangle$ )

polymer backbone of zinc sulfonated EPDM, which is similar to the interaction involving diene rubbers and reinforcing fillers, as manifested in the lowering of  $\tan \delta$  at  $T_g$ , and (b) the interaction between the ionic groups of

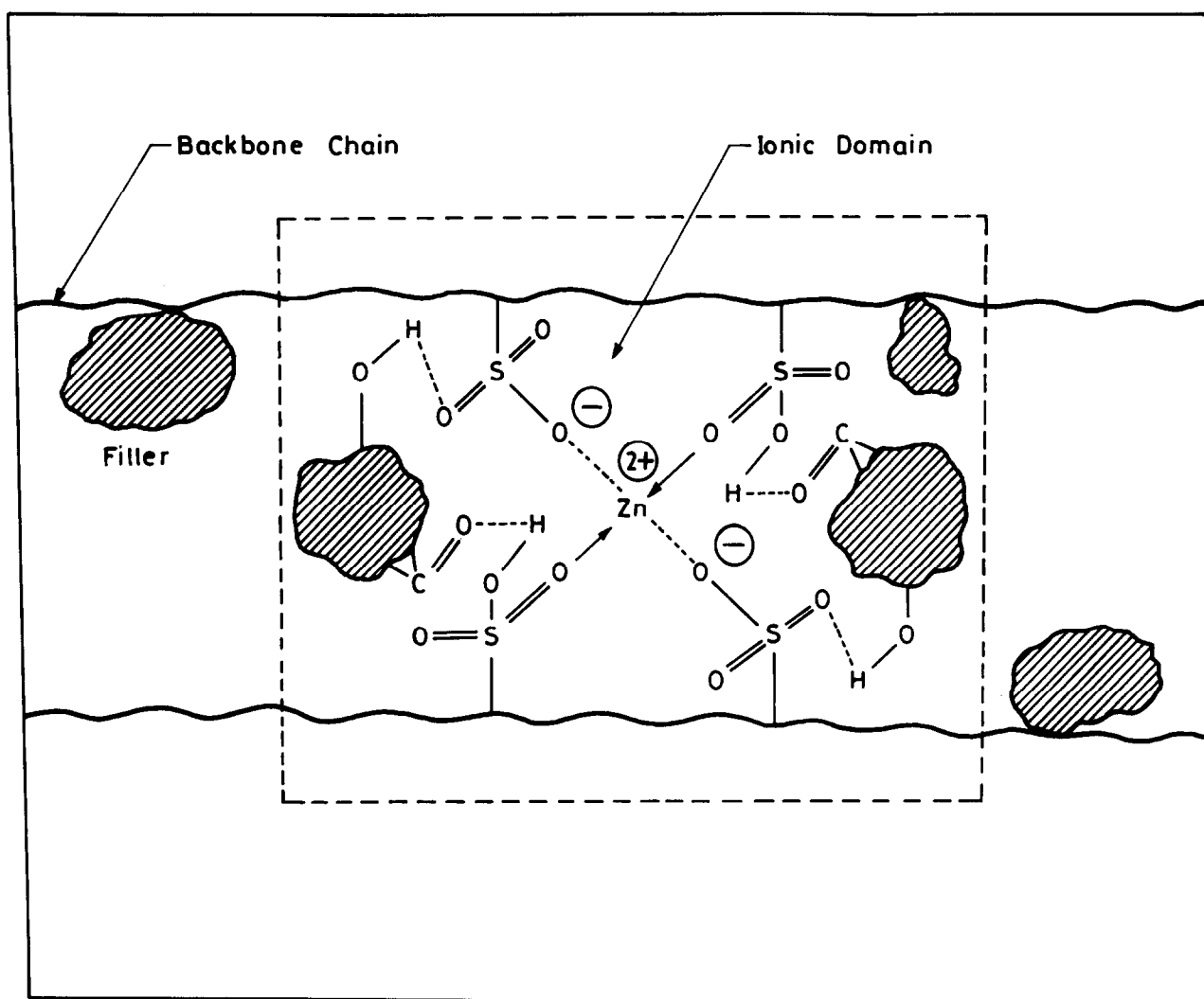


Figure 9 Schematic representation of the interaction between zinc sulfonated EPDM and carbon black

the polymer and the polar groups ( $-\text{OH}$ ,  $>\text{C}=\text{O}$ , etc.) present on the surface of the filler particles, which is manifested in an increase in  $\tan \delta$  at  $T_i$ . While the rubber–filler interaction involving the non-polar polymer backbone is of weak Van der Waals' type, the same due to ionic aggregates can be of much stronger type, as proposed in Figure 9.

Results of dielectric thermal analyses are shown in Figure 10, which depicts the variation of  $\tan \delta$  with temperature for EPDM and zinc sulfonated EPDM. In the case of EPDM the transition at  $115^\circ\text{C}$  is due to the melting of the crystalline zone of the polyethylene block. However, zinc sulfonated EPDM shows two transitions, one at  $123^\circ\text{C}$  and the other at a lower temperature ( $57^\circ\text{C}$ ). While the high temperature transition is believed to be due to the melting of the crystalline polyethylene block, the low temperature transition is believed to be due to the ionic aggregates<sup>20–22</sup>.

Figure 11 shows the frequency dependence of the  $\log(\tan \delta)$  versus temperature plots obtained from the dielectric thermal analyses of zinc sulfonated EPDM and its compounds containing HAF carbon black. It was observed that the compounds containing carbon black exhibit both the transitions, found in the case of the neat zinc sulfonated EPDM.

The thermal activation of dipolar relaxation generally follows the well known Arrhenius law, where activation energy for the relaxation ( $E_{\text{act}}$ ) can be calculated from the slope in the plot of  $\log f$  versus  $1/T_{\text{max}}$ , where  $f$  represents the frequency and  $T_{\text{max}}$  represents the temperature corresponding to the maximum in  $\log(\tan \delta)$  in the plot of  $\log(\tan \delta)$  versus temperature at any frequency<sup>23,24</sup>. Figure 12 shows the Arrhenius plots of  $\log(\text{frequency})$  versus  $1/T_{\text{max}}$ . Since the Arrhenius plots

Table 3 Activation energy for ionic transition from dielectric thermal analysis studies

Sample	Activation energy <sup>a</sup> (kcal mol <sup>-1</sup> )	
	Frequency 1–100 Hz	Frequency 1000–100 000 Hz
Zinc sulfonated EPDM (SE)	90.9	54.1
SE + 10 phr filler	98.4	78.2
SE + 20 phr filler	130.5	101.8
SE + 35 phr filler	181.7	98.5

<sup>a</sup> Calculated from the plots of  $\log(\text{frequency})$  versus  $1/T_{\text{max}}$

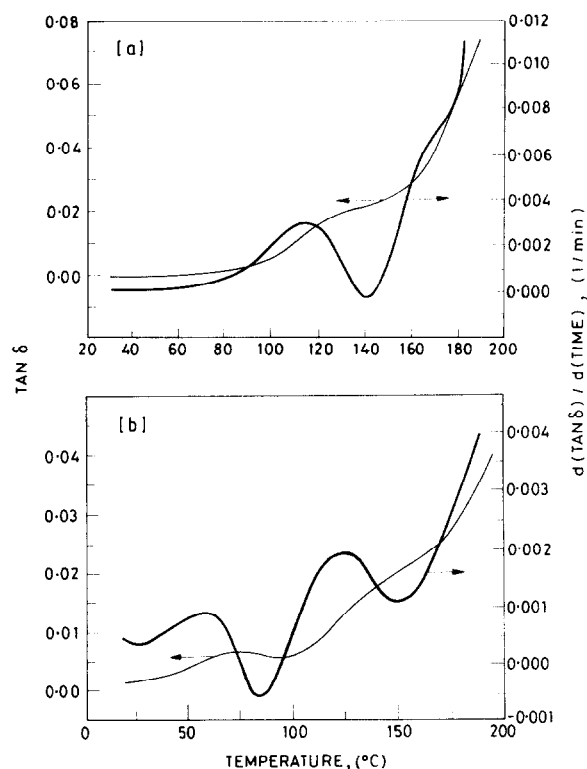


**Figure 10** Semilogarithmic plots of dielectric loss tangent ( $\tan \delta$ ) versus temperature for: (a) EPDM at 1 Hz and (b) zinc sulfonated EPDM at 100 Hz

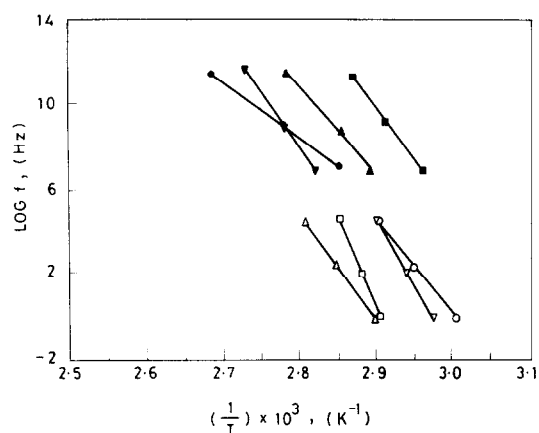


**Figure 12** Plots of  $\log(\text{frequency})$  versus  $1/T_{\max}$  for zinc sulfonated EPDM ( $\circ, \bullet$ ), zinc sulfonated EPDM + 10 phr filler ( $\Delta, \blacktriangle$ ), zinc sulfonated EPDM + 20 phr filler ( $\nabla, \blacktriangledown$ ) and zinc sulfonated EPDM + 35 phr filler ( $\square, \blacksquare$ ). Frequency range 1–100 Hz ( $\circ, \Delta, \nabla, \square$ ) and 1000–100 000 Hz ( $\bullet, \blacktriangle, \blacktriangledown, \blacksquare$ )

show two slopes, it can be inferred that two types of ionic transitions exist, one occurring in the frequency range 1 to 100 Hz and the other occurring in the frequency range 1000 to 100 000 Hz. The activation energy of the ionic transitions calculated from the slopes of the Arrhenius plots are given in Table 3. The transitions at lower frequencies show higher activation energy than those at higher frequencies.

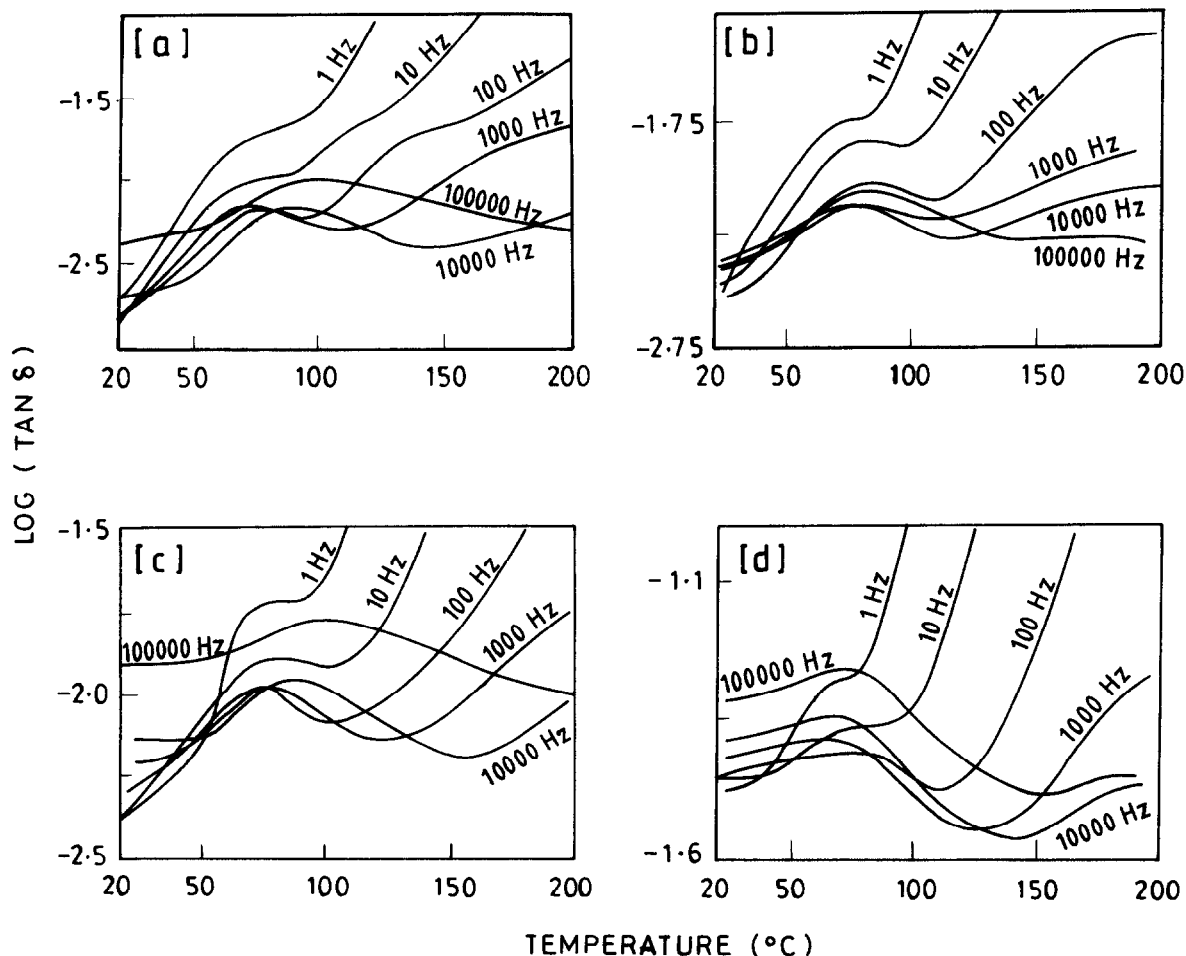


**Figure 11** Frequency dependence of dielectric  $\log(\tan \delta)$  versus temperature plots of: (a) zinc sulfonated EPDM, (b) zinc sulfonated EPDM + 10 phr filler, (c) zinc sulfonated EPDM + 20 phr filler and (d) zinc sulfonated EPDM + 35 phr filler



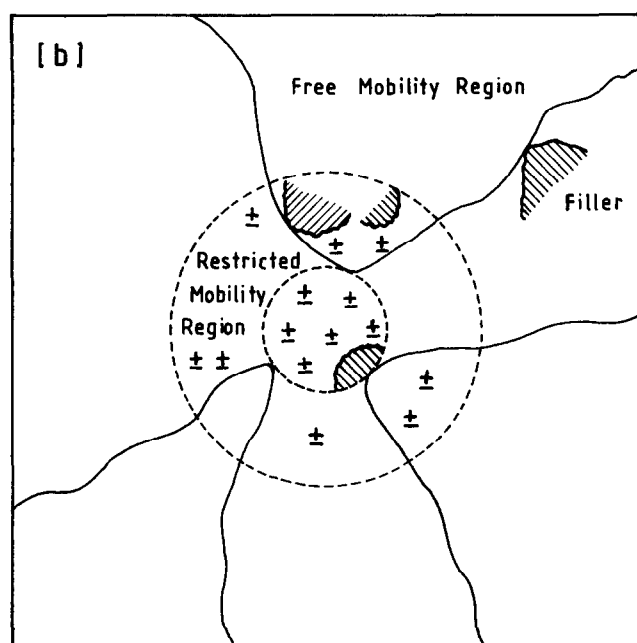
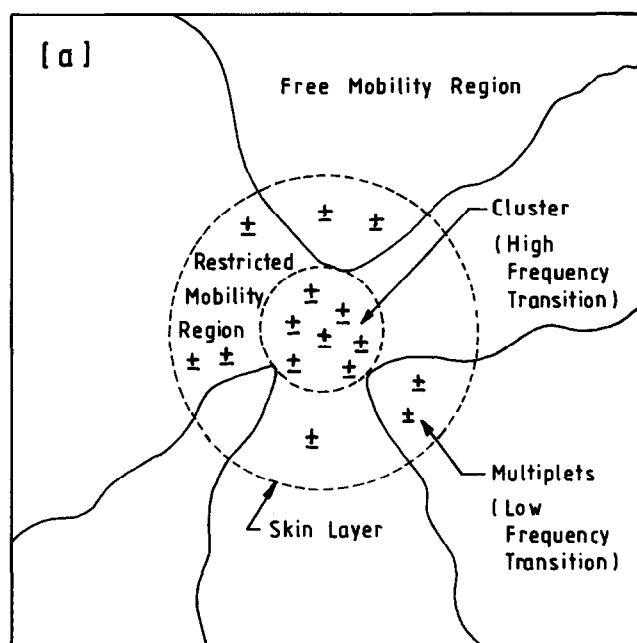


**Figure 13** Schematic diagrams showing (a) the influence of multiplets and clusters on the dielectric relaxation of zinc sulfonated EPDM and (b) the interaction between the filler particles and the ionic aggregates

These observations can be explained on the basis of the 'shell-core model' for the distribution of salt groups in ionomers<sup>25-27</sup>. This model postulates the existence of clusters with a radius of  $\sim 0.1$  nm, in the dry state. The cluster is shielded from the surrounding matrix ions by a shell of hydrocarbon chains. The matrix ions are attracted into the cluster by electrostatic forces, but they cannot approach the cluster more closely than the outside of the hydrocarbon shell. The matrix ions associate to form multiplets, which act as ionic crosslinks and affect the properties of the matrix. The low frequency transitions for ionic groups at low temperatures, which were observed to occur in the case of zinc

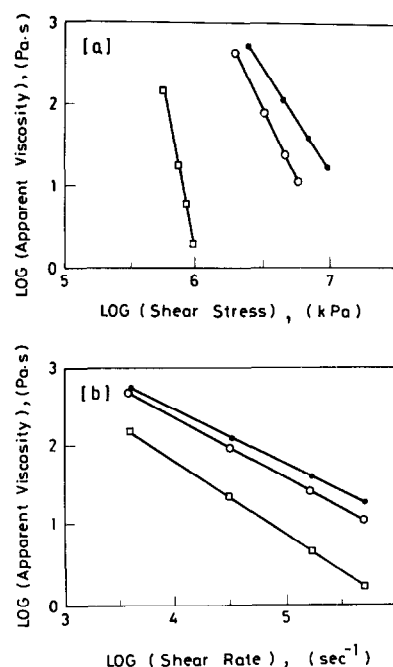


**Figure 14** Apparent viscosity versus (a) shear stress and (b) shear rate at 170°C of EPDM ( $\square$ ), zinc sulfonated EPDM ( $\circ$ ) and zinc sulfonated EPDM + 35 phr HAF carbon black ( $\bullet$ )

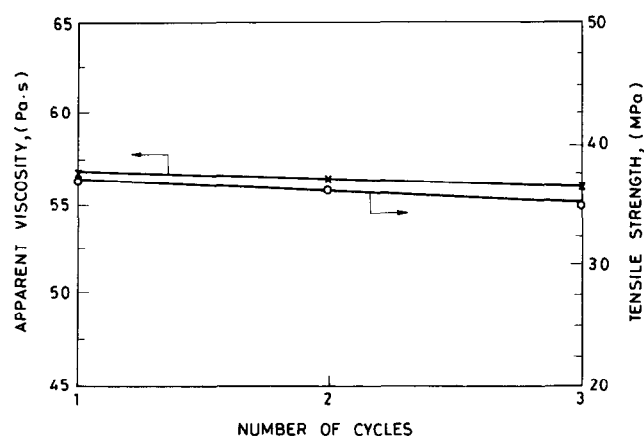


**Figure 15** Apparent viscosity at 170°C and tensile strength of the extrudate at 25°C for zinc sulfonated EPDM containing 35 phr HAF carbon black at different cycles of extrusion

sulfonated EPDM, might be attributed to the polar groups (multiplets) present in the matrix and the high frequency transition occurring at higher temperatures might be originating from the larger aggregates (clusters)<sup>28</sup>, as proposed in Figure 13a. In the presence of carbon black the activation energy of both the low frequency and high frequency transitions increased. Although the reason for such a behaviour is not fully understood, it is apparent that the filler strengthens the multiplets and clusters present in the zinc sulfonated EPDM, presumably by interaction between the ionic groups of the polymer and the polar groups present on the surface of the filler particles as depicted in Figure 13b. The mechanism of the interaction has been shown in Figure 9. This may be the reason for higher retention of stress-strain properties at elevated test temperatures in the case of carbon black filled compounds, compared with the neat zinc sulfonated EPDM.

Figure 14 shows the log–log plots of apparent viscosity versus shear stress and shear rate. The reduction in viscosity with increasing shear stress is due to the pseudoplastic nature of the compounds. At all shear stresses and shear rates, zinc sulfonated EPDM shows higher viscosity than the thermoplastic EPDM and the viscosity of zinc sulfonated EPDM increased on addition of carbon black.

Figure 15 shows the variation of apparent viscosity and tensile strength of the extrudate versus the number of cycles of extrusion through the MPT. It was observed that the viscosity of the mix and tensile strength of the extrudate remain almost constant upon repeated pre-heatings and extrusions. This shows that zinc sulfonated EPDM behaves as a thermoplastic elastomer and can be reprocessed by mechanical recycling without deterioration in properties.

## CONCLUSIONS

HAF carbon black increases the hardness, modulus, tear strength, hysteresis and abrasion resistance of the ionic thermoplastic elastomer based on zinc sulfonated EPDM of high ethylene content. Although the room temperature tensile strength of the carbon black filled compounds is similar to the neat polymer, incorporation of the filler improves the retention of stress–strain properties of the polymer at elevated test temperatures. Dynamic mechanical analyses show the occurrence of an ionic transition at high temperature, in addition to  $T_g$ , for both zinc sulfonated EPDM and its carbon black filled compounds. The results indicate stiffening of the polymer matrix by ionic aggregates in zinc sulfonated EPDM, which is further reinforced by incorporation of the carbon black filler. Results of dielectric thermal analyses indicate that the filler reinforces the ionic aggregates present in the ‘multiplets’ and ‘clusters’ of the ionomer, along with the backbone chain. The thermoplastic elastomeric nature of the polymer is evident from the constancy in the apparent viscosity and tensile strength of the extrudates even after three cycles of repeated preheatings and extrusion of the compound through the Monsanto Processability Tester.

## REFERENCES

- 1 Makowski, H. S., Lundberg, R. D., Westerman, L. and Bock, J. in ‘Ions in Polymers’ (Ed. A. Eisenberg), Advances in Chemistry Series 187, American Chemical Society, Washington, DC, 1980
- 2 Agarwal, P. K., Makowski, H. S. and Lundberg, R. D. *Macromolecules* 1980, **13**, 1679
- 3 MacKnight, W. J. and Lundberg, R. D. *Rubber Chem. Technol.* 1984, **57**, 652
- 4 Paeglis, A. U. and O’Shea, F. X. *Rubber Chem. Technol.* 1988, **61**, 223
- 5 Xie, H.-Q., Xu, J. and Zhou, S. *Polymer* 1992, **32**, 95
- 6 Makowski, H. S., Lundberg, R. D. and Bock, J. *US Patent 4 184 988* (assigned to Exxon Research and Engineering Co.), 1980
- 7 Ferrigno, T. H. in ‘Handbook of Fillers and Reinforcements for Plastics’ (Eds H. S. Katz and J. V. Milewski), Van Nostrand Reinhold Company, New York, 1978
- 8 Eisenberg, A. and King, M. in ‘Ion-Containing Polymers’, Academic Press, New York, 1977
- 9 Kraus, G., in ‘Science and Technology of Rubbers’ (Ed. F. R. Eirich), Academic Press, New York, 1978
- 10 Mathew, N. M. and De, S. K. *Polymer* 1982, **23**, 632
- 11 Hird, B. and Eisenberg, A. *Macromolecules* 1992, **25**, 6466
- 12 Reznikovskii, M. M. and Brodskii, G. I. in ‘Abrasion of Rubber’ (Ed. D. I. James), Maclaren & Sons, London, 1967
- 13 Shallamach, A. *Rubber Chem. Technol.* 1968, **41**, 209
- 14 Bulgin, D. and Walters, M. H. in ‘Proc. 5th Int. Rubber Conf.’, Brighton, UK, 1967, p. 445
- 15 Smallwood, H. *Rubber Chem. Technol.* 1945, **18**, 292
- 16 Smit, P. P. A. *Rheol. Acta* 1966, **5**, 277
- 17 Roy, D., Bhowmick, A. K. and De, S. K. *Polym. Eng. Sci.* 1992, **32**, 971
- 18 Kurian, T., Khastgir, D., De, P. P., Tripathy, D. K. and De, S. K. *Polymer* in press
- 19 Mondal, U. K., Tripathy, D. K. and De, S. K. *Polymer* 1993, **34**, 3832
- 20 Yano, S., Nagao, N., Hattori, M., Hirasawa, E. and Tadano, K. *Macromolecules* 1992, **25**, 368
- 21 Shinichi Yano, S., Tadano, K., Nagao, N., Kutsumizu, S., Tachino, H. and Hirasawa, E. *Macromolecules* 1992, **25**, 7168
- 22 MacKnight, W. J., McKenna, L. W. and Read, B. E. *J. Appl. Phys.* 1968, **38**, 4208
- 23 Blythe, A. R. ‘Electrical Properties of Polymers’, Cambridge University Press, 1979
- 24 Chaki, T. K. and Khastgir, D. *Angew. Makromol. Chem.* 1990, **184**, 55
- 25 MacKnight, W. J., Taggart, W. P. and Stein, R. S. *J. Polym. Sci. Polym. Symp.* 1974, No. 45, 113
- 26 Roche, E. J., Stein, R. S. and MacKnight, W. J. *J. Polym. Sci., Polym. Phys. Edn.* 1980, **18**, 1035
- 27 Fujimura, M., Hashimoto, T. and Kawai, H. *Macromolecules* 1982, **15**, 136
- 28 Bazuin, C. G. and Eisenberg, A. *Ind. Eng. Chem. Prod. Res. Dev.* 1981, **20**, 271